

CIV and CIII] reverberation mapping of PG 1247+267

M. Perna¹, D. Trevese², F. Vagnetti³, F.G. Saturni^{1,4} and M. Dadina⁵

¹ DIFA, Università di Bologna, viale Berti Pichat 6/2, 40127 Bologna, Italy

² Dipartimento di Fisica, Università di Roma La Sapienza, Piazzale Aldo Moro, 5, 00185 Roma, Italy

³ Dipartimento di Fisica, Università di Roma Tor Vergata, Via della Ricerca Scientifica 1, 00133 Roma, Italy

⁴ European Southern Observatory, Karl-Schwarzschild-Strasse 2, 85748 Garching bei Munchen, Germany

⁵ INAF-IASF Bologna, Via Gobetti 101, 40129 Bologna, Italy



CIG grant (eESy)



So far the masses of about 50 active galactic nuclei have been measured through the reverberation mapping technique (RM). Most measurements have been performed for objects of moderate luminosity and redshift, based on H β , which is also used to calibrate the scaling relation which allows single-epoch (SE) mass determination based on AGN luminosity and the width of different emission lines. The SE mass obtained from CIV λ 1549 \AA line shows a large spread around mean values, due to complex structure and gas dynamics of the relevant emission region. Direct RM measures of CIV exist for only 6 AGNs of low luminosity and redshift, and only one luminous quasar (Kaspi et al. 2007). We have collected since 2003 photometric and spectroscopic observations of PG1247+267, the most luminous quasar ever analyzed for RM. We provide light curves for the continuum and for CIV λ 1549 \AA and CIII] λ 1909 \AA , and measures of the reverberation time lags based on the SPEAR method (Zu et al. 2011).

Analysis

In Fig.1 are shown the average and r.m.s. spectra of PG 1247+267, with luminosity $\lambda L_{\lambda}(5100\text{\AA})=10^{47} \text{ erg s}^{-1}$, and redshift $z = 2.04$. Details of the data acquisition and reduction are described in Trevese et al. (2007).

Continuum, CIV and CIII] light curves obtained from spectrophotometry are shown in Fig.2; direct R and V band photometry independent measures of the quasar luminosity changes are also included in the continuum light curve.

We adopt a methodology, called Stochastic Process Estimation for AGN Reverberation (SPEAR), developed by Zu et al. (2011). It makes use of interpolation, which is essential given the small number of data points, using a damped random walk (DRW) model: the entire dataset contributes to each interpolated point, through weights which are statistically determined from the correlation functions of the data. Moreover, statistical uncertainties are assigned to each interpolated value. SPEAR assumes that the emission line variations $l(t)$ are a scaled, smoothed, and delayed version of the continuum variations $c(t)$, obtained through the transfer equation,

$$l(t) = \int dt' \Psi(t') c(t - t')$$

with a simple "top hat" transfer function $\Psi(t)$

$$\Psi(t) = A/\Delta, \quad |t - \tau| \leq \Delta;$$

$$\Psi(t) = 0, \quad \text{elsewhere,}$$

where A , τ and Δ represent the attenuation, the line-continuum lag, and the temporal width of the "top hat" function, respectively.

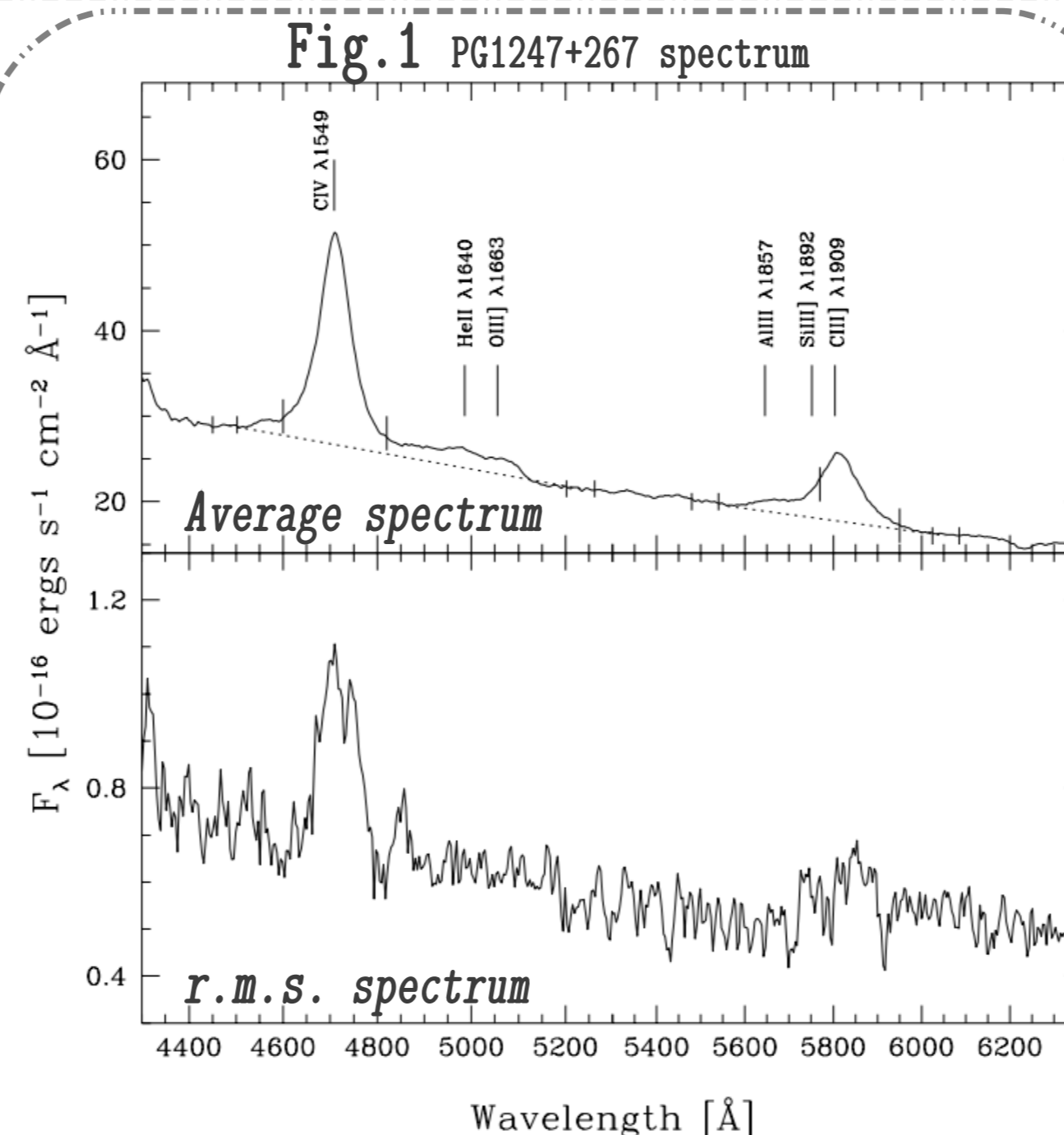


Fig.1 PG1247+267 spectrum
(Upper panel) Average spectrum from our observations. Spectral ranges selected for the determination of the local continua (short ticks) and for the line flux (long ticks) are marked on the spectrum. Dotted lines represent the interpolated local continuum. (Lower panel) r.m.s. spectrum as defined in Peterson et al. (1998)

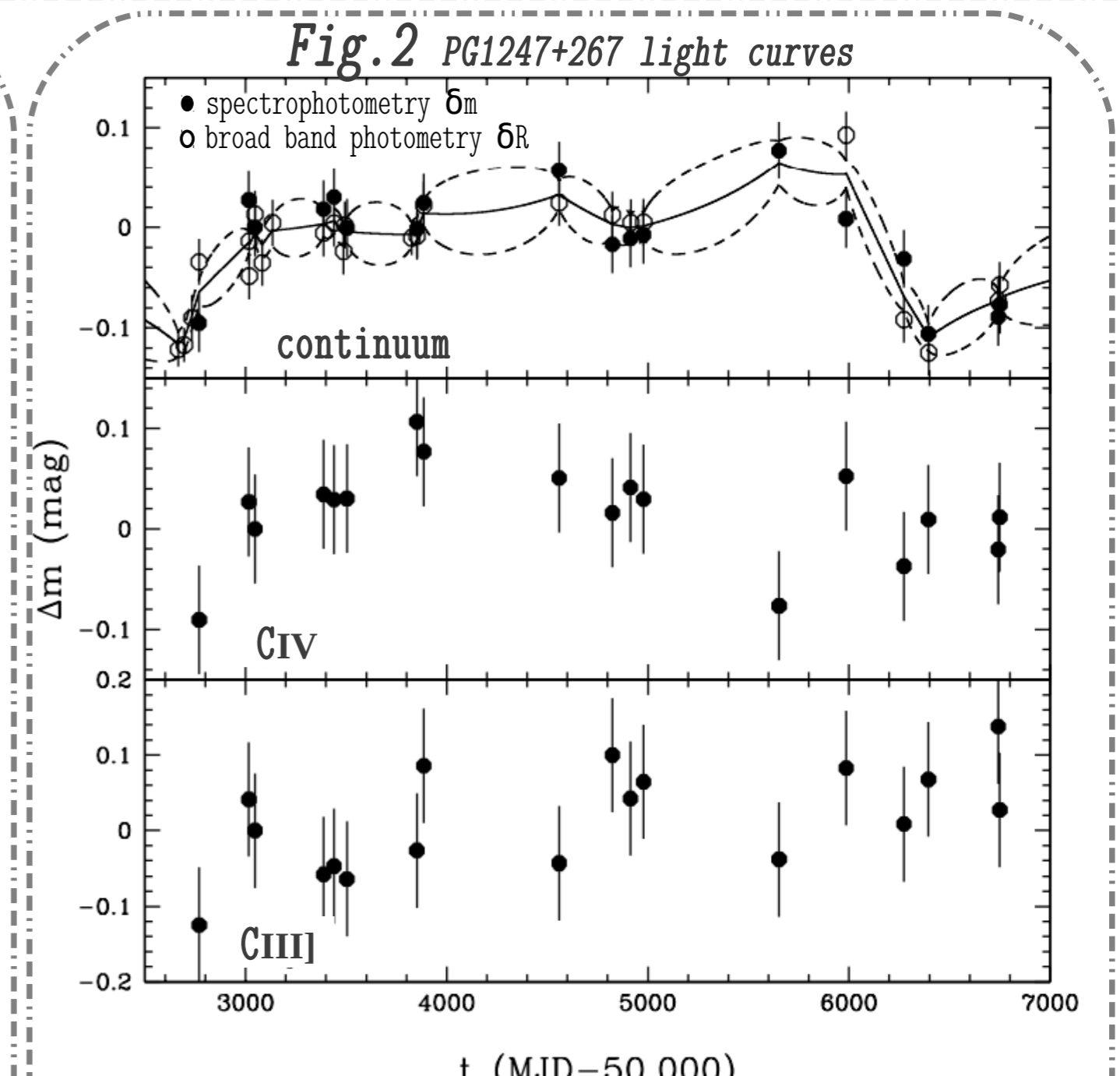


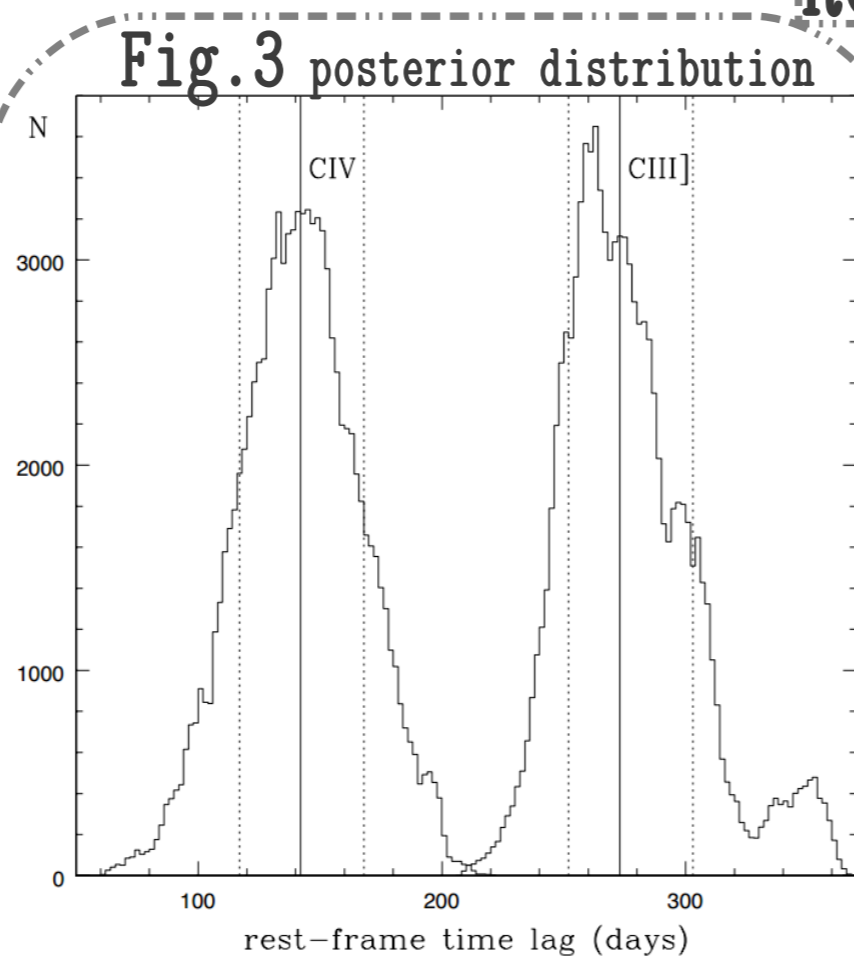
Fig. 2 shows light curves in the observer's frame, for emission lines and continuum, expressed in terms of the relative magnitude variations Δm , with respect to the reference epoch where the absolute calibration was performed. DRW interpolation of the continuum light curve (solid line) and the relevant 1- σ uncertainty (dashed lines) are shown.

Results

With respect to our preliminary results (Perna et al. 2014, awarded with the "COSPAR Outstanding Paper Award For Young Scientists"), the present analysis differs because: i) we fit simultaneously both CIV and CIII] light curves, ii) the continuum light curve includes the available V and R band photometry, and iii) we have included three most recent epochs. Deriving simultaneously the lags of multiple emission lines, SPEAR provides more stringent constraints, which allows better choice among the local likelihood maxima in the space of parameters of the fitting procedure. In addition, SPEAR provides statistical confidence limits on all estimated parameters, through a MCMC method.

In Fig. 3 are shown the relevant posterior distributions obtained for $\tau_{\text{CIII]}}$ and τ_{CIV} . The estimated lags, in rest-frame, are

$$\tau_{\text{CIV}} = 142^{+26}_{-25} \text{ days}, \quad \tau_{\text{CIII]}} = 273^{+30}_{-21} \text{ days}$$



Posterior distributions obtained for τ_{CIV} and $\tau_{\text{CIII]}}$, with the uncertainties defined by the 68% confidence intervals

The time lags are tentative and must be considered with care, due to the still small number of observations. However they seem to be consistent because:

(1) The sizes of the line emission regions are in a ratio $R_{\text{CIII]}}/R_{\text{CIV}} \approx 2$, similar to the case of Seyfert galaxies (see Fig. 4), indicating for the first time a similar ionization stratification in a luminous quasar and low luminosity nuclei.

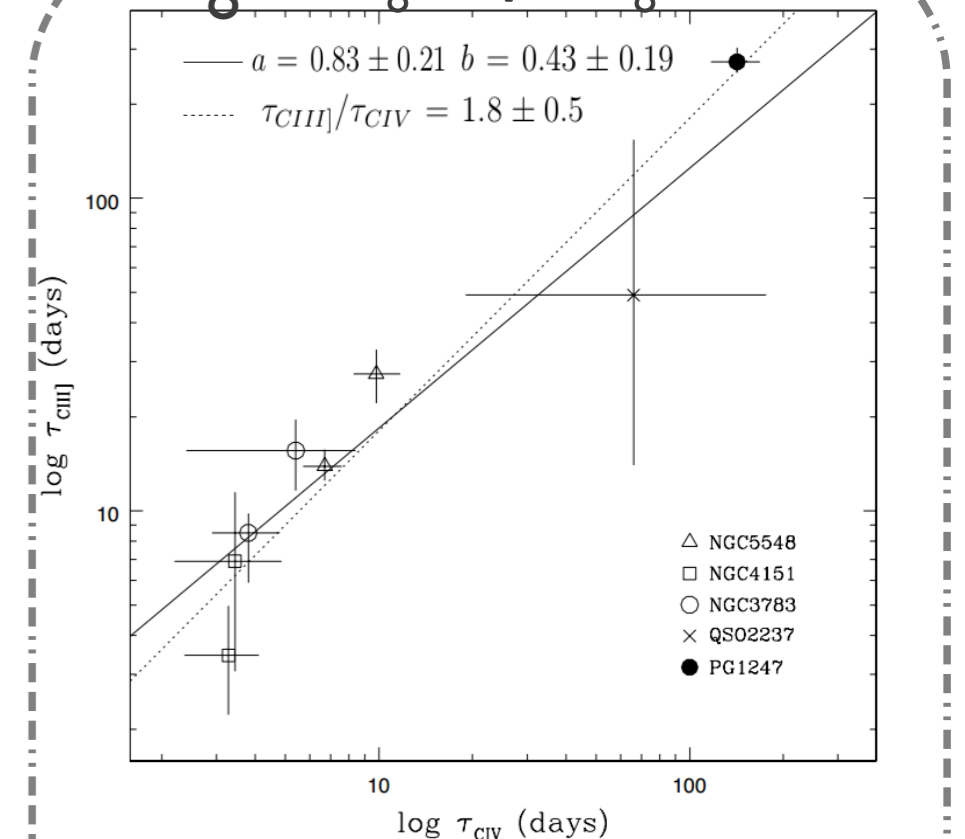
(2) Montecarlo simulations with mock random light curves, and the same sampling pattern, do not produce likelihood maxima in the same region of the parameters space;

(3) Virial black hole mass computed for CIV and CIII] emission lines provide consistent results:

$$M_{\text{BH}} \sim 6.7^{+5.0}_{-1.1} 10^8 M_{\odot} \quad (\text{CIV})$$

$$M_{\text{BH}} \sim 10.5^{+17.2}_{-9.1} 10^8 M_{\odot} \quad (\text{CIII]})$$

Fig.4 $\log \tau_{\text{CIII]}} = a \log \tau_{\text{CIV}} + b$



Reverberation time lags $\tau_{\text{CIII]}}$ versus τ_{CIV} for NGC 5548, NGC 3783, NGC 4151, QSO 2237+0305, PG 1247+267 (our estimate). Linear fits: solid line with two free parameters, dotted line with fixed unitary slope.

Conclusions

Due to relatively small broad line region size and relatively narrow line widths measured (FWHM= 4939 km/s and 5224 km/s for CIV and CIII] respectively), we estimate a small black hole mass. Assuming that the measured $\tau_{\text{CIII]}}$ and τ_{CIV} are real (see sect. Results), this implies:

- a decrease of about about 10% of the slope of the relevant R-L relation (Fig. 5) although the significance of this decrease is still marginal, due to the relatively large dispersion of points and the very small number of CIV RM available to date;
- an anomalously high Eddington ratio, of ≈ 10 . Even the SE mass estimate, which is independent of reverberation lag, produces an Eddington ratio in the range 1.2 – 3.

In Trevese, Perna et al. (2014; accepted to ApJ), we discuss the possibility that either the shape of the emission region (see Runnoe et al. 2014) or an amplification of the luminosity caused by gravitational lensing may be in part responsible of the result.

References:

* Kaspi et al. 2007, ApJ, 659, 997

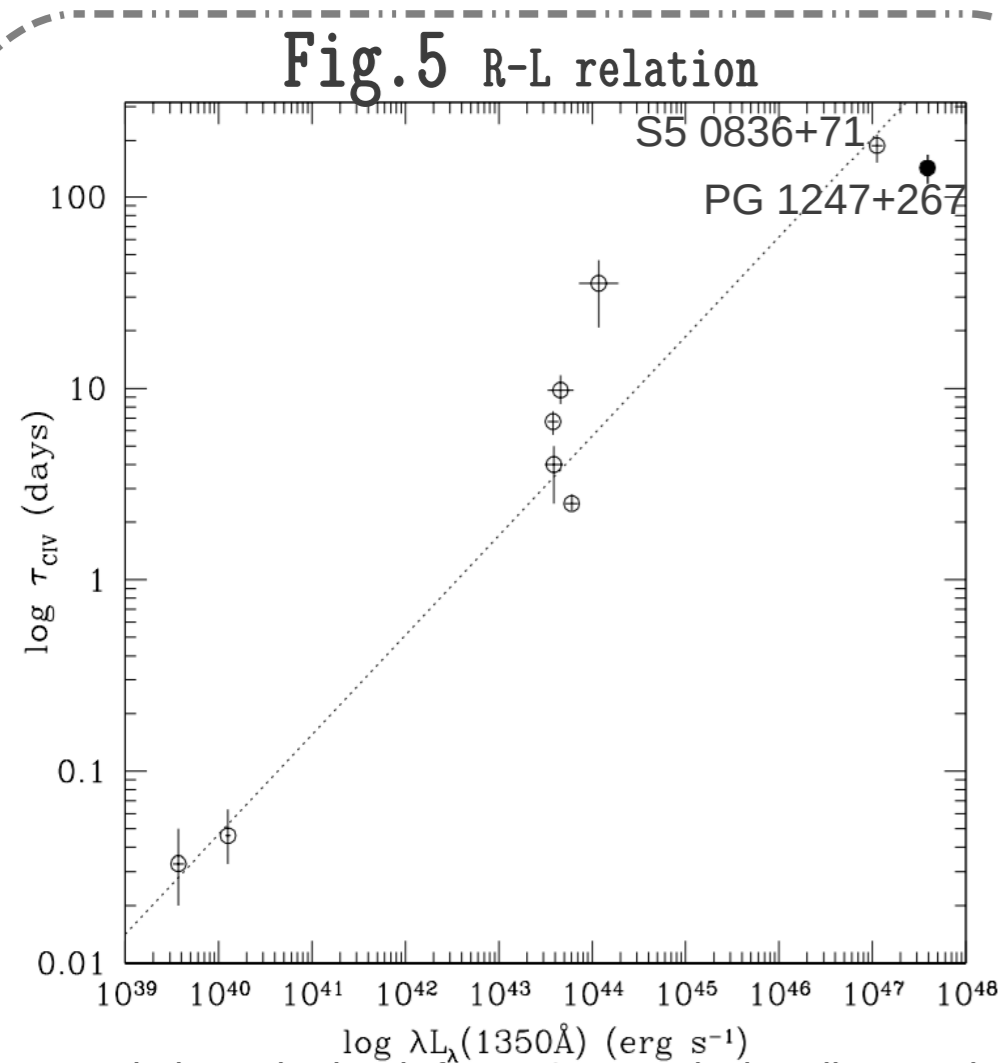
* Peterson et al. 1998, ApJ, 501, 82

* Trevese et al. 2007, A&A, 470, 491

* Perna et al. 2014, AdSpR, 54, 1429P (COSPAR award)

* Runnoe et al. 2014, MNRAS, 438, 3263

* Zu et al. 2011, ApJ, 735, 80



R-L relation obtained from CIV emission line and UV continuum. The dotted line represents the linear fit obtained by Kaspi et al. (2007) with the FITEXY method.